http://dx.doi.org/10.5012/bkcs.2013.34.5.1494

# Energy Flow and Bond Dissociation of Vibrationally Excited Toluene in Collisions with $N_2$ and $O_2$

**Jongbaik Ree,* Sung Hee Kim, and Sang Kwon Lee**

*Department of Chemistry Education, Chonnam National University, Kwangju 500-757, Korea. *E-mail: jbree@jnu.ac.kr*
*Received February 12, 2013, Accepted February 26, 2013*

Energy flow and C-$H_{methyl}$ and C-$H_{ring}$ bond dissociations in vibrationally excited toluene in the collision with $N_2$ and $O_2$ have been studied by use of classical trajectory procedures. The energy lost by the vibrationally excited toluene upon collision is not large and it increases slowly with increasing total vibrational energy content between 5,000 and 45,000 $cm^{-1}$. Intermolecular energy transfer occurs via both of *V-T* and *V-V* transfers. Both of *V-T* and *V-V* transfers increase as the total vibrational energy of toluene increases. When the total energy content $E_T$ of toluene is sufficiently high, either C-H bond can dissociate. The C-$H_{methyl}$ dissociation probability is higher than the C-$H_{ring}$ dissociation probability, and that in the collision with $N_2$ is larger than with $O_2$.

**Key Words :** Collision-induced, Energy transfer, Toluene, Dissociation

## Introduction

The collision-induced relaxation of vibrationally excited polyatomic molecules has a large influence on many chemical processes and it has been the subject of continuing interest in chemistry and physics for the past several decades.[1-17] Molecules highly excited to near their dissociation threshold can undergo bond dissociation and vibrational relaxation, processes that play an important role in reaction dynamics. Most of experimental studies have been carried out using time-resolved infrared flourescence (TR-IRF)[2-4] or ultraviolet absorption (UVA).[5-8] Several studies have been employed by techniques based on photothermal processes.[9-11] Recently, Hsu *et al.* have studied the energy transfer of highly vibrationally excited molecules using crossed-beam/time-of-flight mass spectrometer in combination with time-sliced velocity map ion imaging techniques.[17] Theoretical investigations of polyatomic molecule energy transfer have lagged behind the experimental studies.[18-26]

Recent studies[27-33] show that when the excited molecule is a large organic molecule, the average amount of energy transfer per collision is not very large. Among such large molecules, toluene is a particularly attractive molecule for studying collision-induced energy flow and bond dissociation. Hippler and co-workers carried out a very complete study, investigating the deactivation of the excited toluene by about 60 different collider gases by using the UVA techniques to follow the collisional deactivation of cycloheptatriene.[34] In that experiment the toluene molecules were prepared with 52,000 $cm^{-1}$ of vibrational excitation after irradiation of the cycloheptatriene, which undergoes fast internal conversion and subsequent molecular isomerization to form the highly excited toluene. At this high energy the toluene molecule can further dissociate into benzyl radicals and H atoms.[34] Toselli and co-workers investigated the collisional loss of vibrational energy from gas-phase toluene by 20 collider gases by monitoring the TR-IRF from the C-H stretch modes near 3.3 μm.[25]

Wright and co-workers reported the low temperature measurements on the collisional relaxation of toluene molecules initially containing high amounts of internal excitation.[27] Bernshtein and Oref deal with collisional energy transfer (CET) between aromatic polyatomic molecules including toluene by theoretically.[35]

The purpose of this paper is to study the collision-induced dynamics of highly vibrationally excited toluene interacting with $N_2$ and $O_2$ using quasiclassical trajectory calculations. When the molecule is highly vibrationally excited, the important problems are the determination of energy loss as a function of vibrational excitation and the extent of bond dissociation on collision. The problem of energy loss involves studying energy transfer between the incident particle and toluene through a vibration-to-translation (*VT*) and vibration-to-vibration (*VV*), whereas the problem of intramolecular energy flow focuses on elucidating vibration-to-vibration (*VV*) energy transfer between stretches and bends. Either ring C-H or methyl C-H may dissociate and the efficiency of each bond dissociation can sensitively depend upon the amount and distribution of the initial vibrational excitation. Using the results obtained in the calculations, we will discuss the relaxation and dissociation of the excited CH vibration, and compare the differences of both systems, that is, toluene with $N_2$ and $O_2$.

## Interaction Model and Energies

The model for the toluene-$N_2$ interaction and vibrational coordinates of toluene are defined in Figure 1. In Figure 1(a), we define all 39 intramolecular coordinates of the planar ring needed to be included in the present study. In Figure 1(b), we define the interaction coordinates between the methyl CH bond and the adjacent ring CH bond of a non-

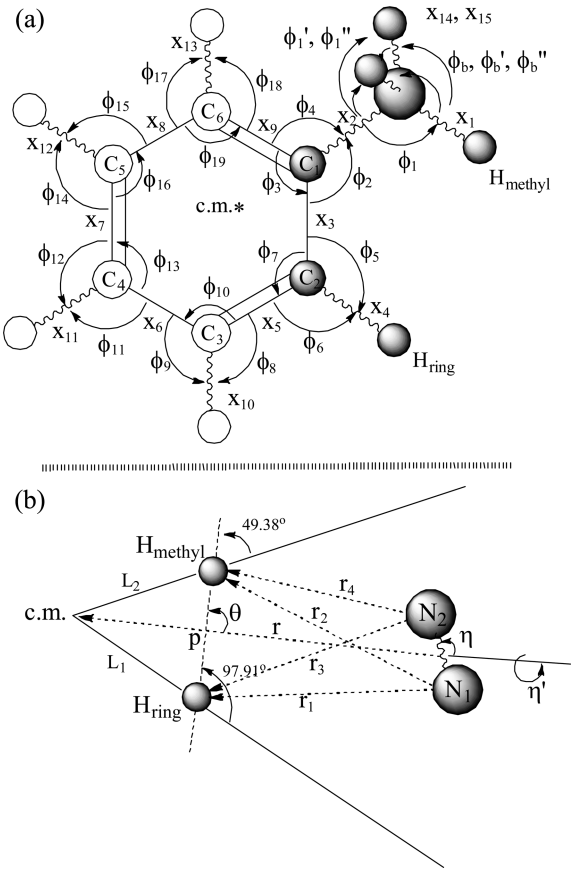


**Figure 1.** Collision model. (a) The stretching and bending coordinates of vibrations included in the model. All carbon atoms and ring H atoms are coplanar and modes are numbered clockwise. The star denotes the center-of-mass (c.m.) of toluene. For convenience we identify each vibration by its displacement (*e.g.*, $x_1$ for $x_{e1} + x_1$). (b) The relative coordinate between $N_2$ and the cm of toluene ($r$).

rotating toluene with the incident $N_2$ molecule. The $CH_{ring}$ bond is in the clockwise side from $CH_{methyl}$. We include 6 stretches ($x_1$, $x_2$, $x_3$, $x_4$, $x_{14}$, $x_{15}$) and 12 bends ($\phi_1$, $\phi_2$, $\phi_3$, $\phi_4$, $\phi_5$, $\phi_6$, $\phi_7$, $\phi_{1'}$, $\phi_{1''}$, $\phi_b$, $\phi_{b'}$, $\phi_{b''}$) in the interaction zone where the $CH_{methyl}$ and $CH_{ring}$ bonds are in direct interaction with $N_2$. We then include the $x_5$~$x_9$ $(CC)_{ring}$ stretches, $x_{10}$~$x_{13}$ $(CH)_{ring}$ stretches and $\phi_8$~$\phi_{19}$ bends around the carbon atoms $C_3$, $C_4$, $C_5$ and $C_6$, a total of 9 stretches and 12 bends, in the inner zone of the molecule.

The important step in developing an interaction potential model is to start with physically reasonable interaction potential energies, which are dependent on the pertinent collision coordinates. The interaction energies needed to describe the collision of $N_2$ with toluene must contain terms responsible for the coupling of the relative motion with the ring C-H stretch and methyl group C-H stretch as well as the coupling between the stretches and bends. We first introduce the interatomic distances $r_1$~$r_4$ in the interaction model defined in Figure 1(b), where $r$ represents the distance between center-of-mass (c.m.) of $N_2$ and the c.m. of toluene describing the relative motion of the collision system. The interatomic distances can be expressed in terms of the instantaneous coordinates of the C-$H_{methyl}$ bond, C-$CH_{methyl}$ bond, $(C\text{-}C)_{ring}$ bond, C-$H_{ring}$ bond, $CCH_{methyl}$ bend, $CCC_{methyl}$ bend, $CCH_{ring}$ bend and N-N bond. That is, $r_i = r_{ei} + x_i$ ($r$, $x_1$, $x_2$, $x_3$, $x_4$, $\phi_1$, $\phi_2$, $\phi_5$, $x$, $\theta$) for $i$ = 1-4, where $x$ is the displacement of the N-N from its equilibrium bond distance $d$, and $\theta$ is the angle of incidence defined in Figure 1(b). The coupling of these modes with others including those of the inner zone will have to be considered in formulating the overall interaction energy. The values of equilibrium bond distances and other potential parameters for toluene are listed in Table 1 of Ref. 32. Each bond length will be denoted by ($x_{ei} + x_i$), where $x_i$ is the displacement of the bond length from its equilibrium value $x_{ei}$. Similarly, we express each bending coordinate as ($\phi_{ej} + \phi_j$), where $\phi_j$ is the displacement of the $j$th bending vibration from the equilibrium angle $\phi_{ej}$.

The $N_1$-to-$H_{ring}$($r_1$), $N_1$-to-$H_{methyl}$($r_2$), $N_2$-to-$H_{ring}$($r_3$) and $N_2$-to-$H_{methyl}$($r_4$) interatomic distances can be obtained as

$$r_1 = [V^2 + A^2 - 2VA\cos(\theta - \rho_1)]^{1/2} \quad (1a)$$

$$r_2 = [V^2 + B^2 + 2VB\cos(\theta - \rho_1)]^{1/2} \quad (1b)$$

$$r_3 = [W^2 + A^2 - 2WA\cos(\theta + \rho_2)]^{1/2} \quad (1c)$$

$$r_4 = [W^2 + B^2 + 2WB\cos(\theta + \rho_2)]^{1/2} \quad (1d)$$

where, $V$ and $W$ are distances between $N_1$ and $N_2$ and point "$p$", respectively.

$$V = [(r-z)^2 + \gamma_N^2(d+x)^2 + 2(r-z)\gamma_N(d+x)\cos\eta\cos\eta']^{1/2}, \quad (2a)$$

$$W = [(r-z)^2 + \gamma_N^2(d+x)^2 - 2(r-z)\gamma_N(d+x)\cos\eta\cos\eta']^{1/2}, \quad (2b)$$

Here, $\eta$ and $\eta'$ are the rotational angles of $N_2$, $\gamma_N = m_N/(m_N + m_N)$,

$$z = c_1\sin(99.61^\circ)/\sin\theta,\ A = c_2\sin(\theta - 49.38^\circ)/\sin\theta,$$

$$B = c_1\sin(99.61^\circ - \theta)/\sin\theta$$

$$\rho_1 = \theta - 49.38^\circ,\ \rho_2 = 99.61^\circ - \theta$$

$$c_1 = \left[q^2 + (x_{e4} + x_4)^2 - 2q(x_{e4} + x_4)\cos\left(\frac{2}{3}\pi + \phi_5 + s\right)\right]^{1/2},$$

$$c_2 = [G^2 + (x_{e1} + x_1)^2 - 2G(x_{e1} + x_1)\cos(107.6^\circ + \phi_1 - \xi)]^{1/2},$$

$$G = [0.884 + (x_{e2} + x_2)^2 - 1.880(x_{e2} + x_2)\cos\phi_2]^{1/2},$$

$$q = \left[(x_{3e} + x_3)^2 + 0.884 - 2(x_{3e} + x_3)0.9402\cos\left(\frac{2}{3}\pi + \phi_2\right)\right]^{1/2},$$

$$s = \sin^{-1}\left[\frac{0.9402}{q}\sin\left(\frac{\pi}{3} + \phi_2\right)\right],$$

$$\xi = \sin^{-1}[0.9402\sin\phi_2/G].$$

Here all distances are in Å and $z$ is distance between the c.m. of toluene and point "$p$" between $H_{ring}$ and $H_{methyl}$. For the convenience, it is derived for $N_2$, but N should be replaced by O for toluene+$O_2$ collision.

The above distances and relations determine the coupling

of the translation to vibrational motions (*i.e.*, the coupling of $r$ with $x_1$, $x_2$, $x_3$, $x_4$, $\phi_1$, $\phi_2$, $\phi_5$, and $x$). These $x$'s and $\phi$'s are then coupled with the inner modes indicated in Figure 1(a).

The overall interaction energy is the sum of the Morse-type intermolecular terms, Morse-type stretching terms and the harmonic bending terms of toluene, intramolecular coupling terms, and London interaction,

$$V = \Sigma U(r_\alpha)+U_s(x_i)+U_b(\phi_j)+U_{int}(Y_iY_j) + U_{N_2}(x)+\frac{-3I_1I_2}{2(I_1+I_2)}\frac{\alpha_1\alpha_2}{r^6} \quad (3)$$

Where,

$$U(r_\alpha) = D[e^{(r_{e\alpha}-r_\alpha)/a}-2e^{(r_{e\alpha}-r_\alpha)/2a}],\ \alpha = 1\text{-}4$$

$$U_s(x_i) = \Sigma D_i[1-e^{-x_i/b_i}]^2,\ i = 1\text{-}15$$

$$U_b(\phi_j) = 1/2\Sigma k_j\phi_j^2,\ j = 1\text{-}24$$

$$U_{int}(Y_iY_j) = \sum_{ij} K_{ij}(Y_i-Y_{ei})(Y_j-Y_{ej}),\ i\neq j$$

$$U_{N_2}(x) = D_{N_2}\left[1-e^{-x/b_{N_2}}\right]^2.$$

In London interaction, $I_i$ is the ionization potential and $\alpha$ is the polarizability. For the intermolecular interaction, we take $D = 193.69k_B$ and $215.24k_B$ for toluene+$N_2$ and toluene+$O_2$, respectively, the Lennard-Jones (LJ) parameter for the well depth for the collision pairs calculated by the usual combining rule,[36] where $k_B$ is the Boltzmann constant, and $a = 0.250$ Å and 0.246 for toluene+$N_2$ and toluene+$O_2$, respectively.[36,37] For the $i$th stretch, we use $b_i = (2D_i/\mu_i\omega_i^2)^{1/2}$, where $D_i = D_{o,i} + \frac{1}{2}\hbar\omega_{ei}$, to determine the exponential range parameters listed in Table 1 of Ref. 32. In the coupling terms, $Y_i = x_i$ or $\phi_i$ and the coupling constant $K_{ij}$ are taken from Xie and Boggs' *ab initio* calculations.[38] The potential and spectroscopic constants for the toluene, $N_2$ and $O_2$ are listed in Table 1.[39-41]

In Figure 2, we present the equipotential plot of the overall interaction energy for $N_2$ approaching toluene molecule, which is in its equilibrium geometry. Toluene is oriented and scaled to closely represent the collision configuration and the c.m. of toluene is fixed at the origin of the plot. Here the abscissa is the c.m. of toluene to c.m. of $N_2$ line at $\theta = 90^o$ and the ordinate, which is parallel to the $H_{methyl}$-to-$H_{ring}$ axis, passes through the c.m. of toluene. In Figure 2(a), we show the potential energy surface (PES) for $\phi = 0^o$, which represents the collinear configuration of c.m. of toluene···N–N. The surface is quite symmetric with respect to the two hydrogen atoms. For $r < 3.5$ Å, the interaction energy rises rapidly and the contour lines for this repulsive region are not shown in Figure 2(a). Even though there is a very repulsive region, the $N_2$ molecule can approach very close to the toluene molecule, implying the fact that the incoming $N_2$ molecule perturbs the target significantly and the energy transfer occurs effectively. As the rotational angle of $N_2$ changes to $\phi = 90^o$, the PES becomes unsymmetrical. At this configu-

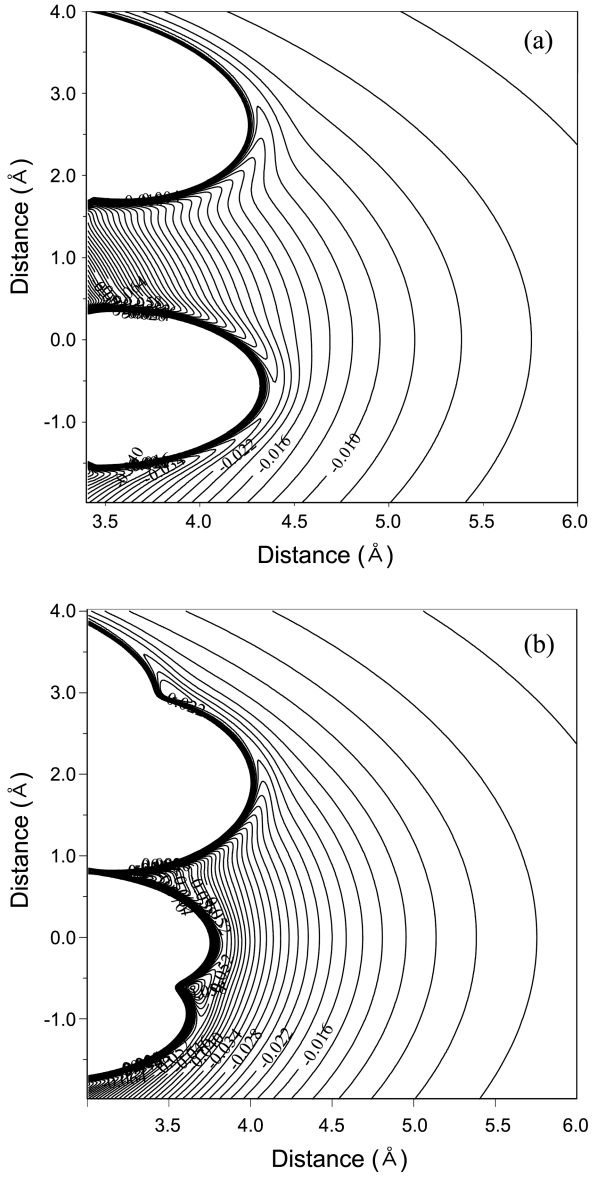


**Figure 2.** The equipotential plot of the interaction energy for $N_2$ interacting with C-$H_{methyl}$ and C-$H_{ring}$ of the fixed toluene from different directions (a) $\eta = 0°$ and (b) $\eta = 90°$. The origin (0,0) of the plot is the c.m. of toluene. The contours are labeled in electron volt and they are in 0.002 eV intervals. The repulsive region is truncated at 0.10 eV.

**Table 1.** Potential and spectroscopic constants for toluene, $N_2$ and $O_2$

| Molecule | toluene | $O_2$ | $N_2$ |
|---|---|---|---|
| Ionization energy, $I$ (eV)[a] | 8.828 | 12.0697 | 15.581 |
| Polarizability, α (Å$^3$) | 9.906[a] | 1.562[b] | 1.710[b] |
| Dissociation energy, $D_{oi}$ (eV)[c] | | 5.116 | 9.759 |
| Bond distance, $d_i$ (Å)[c] | | 1.2075 | 1.098 |
| Vibrational frequency (cm$^{-1}$)[c] | | 1580.19 | 2358.57 |
| Range parameter, $b$ (Å)[d] | | 0.377 | 0.372 |

[a]Reference 39. [b]Reference 40. [c]Reference 41. [d]Range parameter is determined from the relation $b_i=(2D_i/\mu_i)^{1/2}/\omega_i$.

ration, the potential wells of 0.06 eV or 696 $k_B$ appear at three places near $r$ = 3.5 Å from the origin in the direction to two hydrogen atoms and the center of two hydrogen atoms [see Figures 2(b)]. The PES for $O_2$ is very similar to for $N_2$.

The equations of motion which determine the time evolution of the relative motion (trajectory), 15 stretches and 24 bends for the given incident angle θ are

$$\mu d^2r(t)/dt^2 = -\frac{\partial}{\partial r}V(r, x_1, \ldots, x_{15}, \phi_1, \ldots, \phi_{24}, x, \theta), \quad (3a)$$

$$\mu_i d^2x_i(t)/dt^2 = -\frac{\partial}{\partial x_i}V(r, x_1, \ldots, x_{15}, \phi_1, \ldots, \phi_{24}, x, \theta), \quad i = 1\text{-}15 \quad (3b)$$

$$I_j d^2\phi_j(t)/dt^2 = -\frac{\partial}{\partial \phi_j}V(r, x_1, \ldots, x_{15}, \phi_1, \ldots, \phi_{24}, x, \theta), \quad i = 1\text{-}24 \quad (3c)$$

$$\mu_{inc} d^2x(t)/dt^2 = -\frac{\partial}{\partial x}V(r, x_1, \ldots, x_{15}, \phi_1, \ldots, \phi_{24}, x, \theta), \quad (3d)$$

where $\mu$ is the reduced mass of the collision system, $\mu_i$ is the reduced mass associated with the $i$th stretch and $I_j$ is the moment of inertia of the $j$th bend. $\mu_{inc}$ is the reduced mass of incident molecule $N_2$ (or $O_2$). We use the standard numerical routines[42,43] to integrate these equations for the initial conditions at $t = t_0$ and their conjugate quantities $(d/dt)r(t_0)$, $(d/dt)x_i(t_0)$, $(d/dt)\phi_j(t_0)$, and $(d/dt)x(t_0)$, where the derivatives are evaluated at $t = t_0$.

## Numerical Procedures

We sample 40,000 trajectories for each run at 300 K, where the sampling includes determining collision energies ($E$) chosen from the Maxwell distribution. In studying the $E$ dependence of energy transfer and bond dissociation, we carry out the same sampling except that $E$ is now fixed at a specified value. The initial conditions for solving the equations of motion for the relative motion and the displacements and phases for the vibrational motions in the interaction zone are given in Ref. 15. We vary the initial vibrational energies of the C-$H_{ring}$ and C-$H_{methyl}$ bonds (*i.e.*, $i$ = 1 and 4) systematically, while maintaining the rest of the vibrational motions in the ground state. Each vibrational phase is a random number $\delta_i = 2\pi s_i$ with flat distribution of $s_i$ in the interval (0,1). The initial separation between the center of masses of toluene and $N_2$ (or $O_2$) is set as 15 Å, and trajectories are terminated when the separation reaches 50 Å after they passed through the closest distance of approach. The integration was performed with a stepsize of 0.169 fs, which is one-tenth the period of the largest frequency, the ring CH vibration, and is small enough to ensure energy conservation to at least five significant figures along a trajectory. We have also confirmed that the numerical procedure allows the trajectories to be successfully backintegrated.

For such highly excited CH vibrations considered here, the discussion of bond dissociation in terms of normal-mode analysis is not useful since the dissociation does not involve a particular normal mode. From the dynamics study, we can decide when the C-H distance exceeds a critical value, at which time dissociation is assumed to occur. The occurrence of dissociative events can be readily recognized by studying the time evolution of the methyl (or ring) CH bond trajectory and the $CH_{methyl}$ (or $CH_{ring}$) vibrational energy, as well as all intermediate modes in the interaction zone, which are conduits for the energy flow. The bond dissociation probability will be defined as the ratio of the number of dissociative trajectories to the total number of trajectories sampled, which is 40,000, in each run.

We define the ensemble-averaged energy transfer $\langle\Delta E\rangle = \langle E_{final} - E_{initial}\rangle$, the difference between the final and initial translational and vibrational energies of $N_2$ (or $O_2$). Thus, a positive value of $\langle\Delta E\rangle$ represents the ensemble-averaged energy loss by toluene, a $V \rightarrow T$, $V \rightarrow V$ and $V \rightarrow R$ energy transfer processes. We also determine the ensemble average of vibrational energy of each mode consisting of kinetic and potential energy terms in toluene, and then calculate the difference between this average energy and the energy initially deposited in the mode. The dissociation of a highly excited bond occurs when the bond gains energy from the incident molecule ($T \rightarrow V$ or $V \rightarrow V$ pathways) or it gains energy from adjacent bonds through intramolecular energy flow or both. In any event, the energy gained by the bond must exceed the dissociation threshold, which corresponds to the CH bond extension beyond the point of no return, regardless of the excitation pattern. When the bond dissociation occurs, we need to determine energy transfer for dissociative or nondissociative trajectories separately.

## Results and Discussion

**Dependence of Energy Loss on the Total Vibrational Energy Content.** In Figure 3, we show the dependence of energy loss, $-\langle\Delta E\rangle$ on the total vibrational energy content $E_T$ for toluene colliding with $N_2$ at 300 K. The smallest value of $E_T$ considered in this figure is 6,203 $cm^{-1}$ or 0.769 eV, which corresponds to vibrational energies of C-$H_{methyl}$ and C-$H_{ring}$ being 3,057 $cm^{-1}$ (0.379 eV) and 3,145 $cm^{-1}$ (0.390 eV), respectively. That is, both bonds are the first vibrational excited states of each bond. At this total vibrational energy content, the energy loss is 53 $cm^{-1}$ (or 0.0066 eV) [see "sum" in Figure 3(a)]. In this Figure, it is shown three plots those are $V \rightarrow V$, $V \rightarrow T$, and "sum". Here, $V \rightarrow V$ means that the vibrational energies of toluene transfer to the vibrational energy of $N_2$, and $V \rightarrow T$ means the transfer to the translational energy of $N_2$. "Sum" means the sum of $V \rightarrow V$ and $V \rightarrow T$ transfers.

Intermolecular energy transfer occurs *via* both of $V \rightarrow T$ and $V \rightarrow V$ transfers. The $V \rightarrow R$ transfer is not significant because the ensemble-averaged energy loss of toluene to the rotational energy of $N_2$, $\langle\Delta E_{rot}\rangle \lesssim 2$ $cm^{-1}$ over the range of the total vibrational energy content considered here. The magnitude of energy loss "sum" increases gradually as the total vibrational energy content $E_T$ increases, both of $V \rightarrow T$ and $V \rightarrow V$ transfers are gradually increased. As shown in

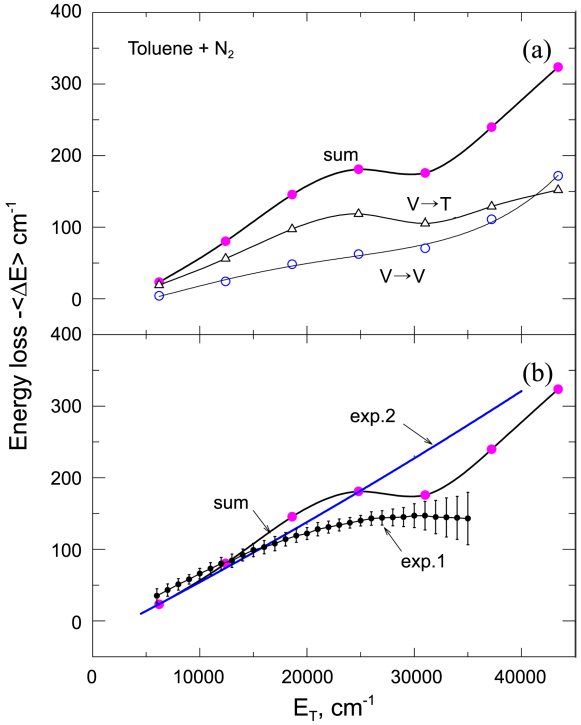


**Figure 3.** Energy loss against the total vibrational energy content $E_T$ for toluene+$N_2$ collision. (a) $V \rightarrow V$ means that the vibrational energies of toluene transfer to the vibrational energy of $N_2$, and $V \rightarrow T$ means the transfer to the translational energy of $N_2$. "Sum" means the sum of $V \rightarrow V$ and $V \rightarrow T$ transfers. (b) Experimental data are taken from Refs. 25 (exp. 1) and 27 (exp. 2).

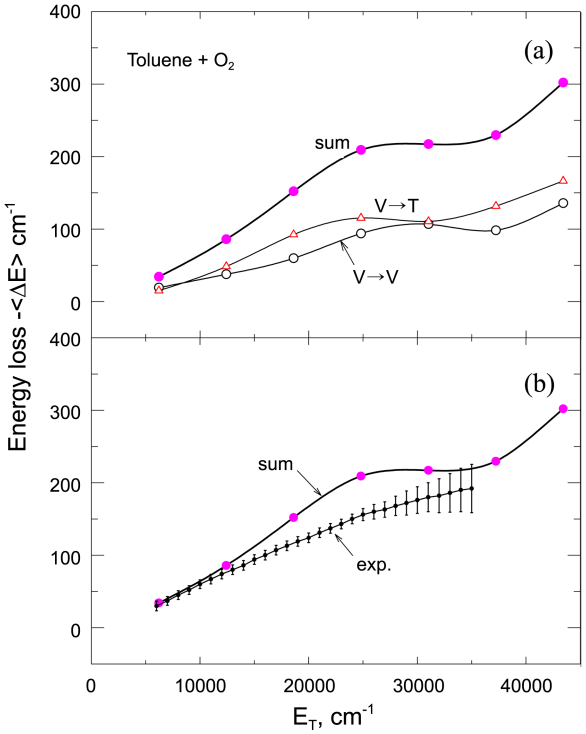


**Figure 4.** Energy loss against the total vibrational energy content $E_T$ for toluene+$O_2$ collision. (a) $V \rightarrow V$, $V \rightarrow T$ and "Sum" are the same meaning as Figure 3. (b) Experimental data are taken from Ref. 25.

Figure 3(a), when $E_T$ is raised from 6,203 cm$^{-1}$ to 43,425 cm$^{-1}$, $-\langle\Delta E\rangle$ increases from 23 cm$^{-1}$ to 324 cm$^{-1}$, which are less than 1% of $E_T$. The latter $E_T$ value, 43,425 cm$^{-1}$ corresponds to C-$H_{methyl}$ and C-$H_{ring}$ having the initial vibrational energies of 21,419 cm$^{-1}$ and 22,006 cm$^{-1}$, respectively. In their study on the toluene–$N_2$ at room temperature, Wright *et al.* found that there is gradual increase in the magnitude of energy loss when the range of the total vibrational energy content is from 5,000 cm$^{-1}$ to about 40,000 cm$^{-1}$ for toluene excited directly by adsorption of photons at 266 nm.[27] Toselli *et al.* also reported the collisional loss of vibrational energy of highly excited toluene in the range from 5,000 cm$^{-1}$ to about 40,000 cm$^{-1}$ by monitoring the time-resolved infrared fluorescence from the C-H stretch modes near 3.3 μm.[25] As shown in Figure 3(b), the $E_T$ dependence and the magnitude of $-\langle\Delta E\rangle$ of the present result below 40,000 cm$^{-1}$ agree fairly well with the observed data. A slow variation of $-\langle\Delta E\rangle$ with increasing $E_T$ shown in Figure 3 has been known to be the general behavior for the relaxation of toluene by rare gases and diatomic molecules such as $N_2$ in experimental and theoretical studies.[25,27,28]

As shown in Figure 4, $-\langle\Delta E\rangle$ for toluene+$O_2$ collision shows the same trend as for $N_2$, and $-\langle\Delta E\rangle$ increases from 34 cm$^{-1}$ to 302 cm$^{-1}$ when $E_T$ is raised from 6,203 cm$^{-1}$ to 43,425 cm$^{-1}$. The $E_T$ dependence and the magnitude of $-\langle\Delta E\rangle$ of the toluene+$O_2$ collision below 40,000 cm$^{-1}$ agree also fairly well with the observed data.[25]

**Bond Dissociation.**

**Dissociation of C-$H_{methyl}$ versus C-$H_{ring}$:** We now discuss the collision-induced dissociation of highly excited toluene molecules. We plot the dissociation probabilities for toluene +$N_2$ collision at 300 K in Figure 5. Here we take both C-H bonds have their initial vibrational energies which are below their respective dissociation threshold by the same amount. When each of them is 1.5 eV or 12,097 cm$^{-1}$ below the threshold, the total vibrational energy content is 47,814 cm$^{-1}$ above the zero point energy with 27,880 cm$^{-1}$ in C-$H_{ring}$ and 19,934 cm$^{-1}$ in C-$H_{methyl}$, the dissociation probabilities are $P_{C\text{-}Hmethyl}$ = 0.00015 and $P_{C\text{-}Hring}$ = 0.0001. Here dissociation probabilities are very small because a large amount of energy has to deposit in one of the bonds. We note that the ensemble-averaged energy loss by toluene for $E_T$ = 47,814 cm$^{-1}$ is only 179 cm$^{-1}$ or 0.0222 eV. Since the C-$H_{methyl}$ (or C-$H_{ring}$) bond is 12,097 cm$^{-1}$ below its dissociation threshold and the molecule loses 179 cm$^{-1}$, this bond has to gain at least 12,097 cm$^{-1}$ from C-$H_{ring}$ (or C-$H_{methyl}$) through intramolecular energy redistribution to dissociate. When the total energy content is increased from 47,814 cm$^{-1}$ toward the dissociation threshold, the probabilities rise very rapidly. When $E_T$ is as high as 70,396 cm$^{-1}$, which corresponds to the vibrational energy of each bond only 0.1 eV below the dissociation threshold, the dissociation probabilities are now $P_{C\text{-}Hmethyl}$ = 0.0262 and $P_{C\text{-}Hring}$ = 0.0333. This indicate that the vibrational motions of a highly excited molecule can be readily perturbed by the incident molecule and need only a small amount of energy to dissociate. When the incident

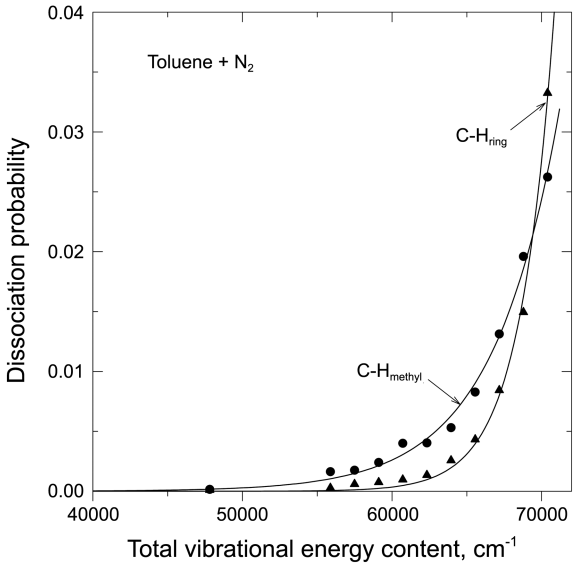


**Figure 5.** Dissociation probabilities of C-$H_{methyl}$ and C-$H_{ring}$ bonds against the total vibrational energy content $E_T$ for toluene+$N_2$ collision.

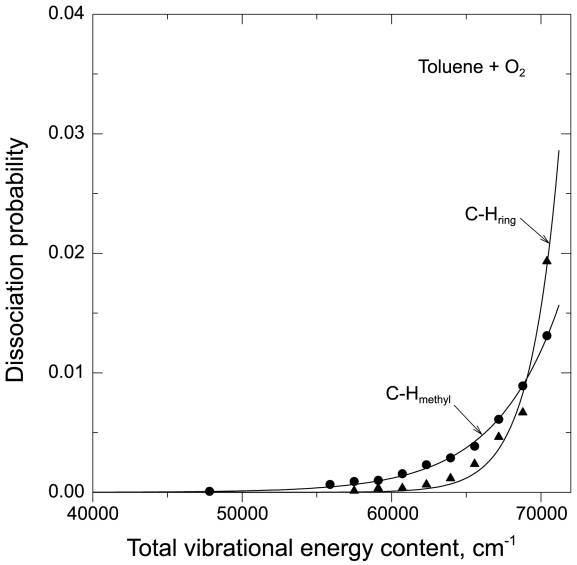


**Figure 6.** Dissociation probabilities of C-$H_{methyl}$ and C-$H_{ring}$ bonds against the total vibrational energy content $E_T$ for toluene+$O_2$ collision.

molecule is $O_2$, the dissociation probabilities are always less than for $N_2$ molecule [see Figures 5 and 6]. Furthermore, as shown in Figures 5 and 6, $P_{C\text{-}Hmethyl}$ is generally greater than $P_{C\text{-}Hring}$ for the total vibrational energy content. We will discuss these differences later in the next section.

In Figure 7, we show the dependence of the dissociation probabilities of C-H bonds for toluene+$N_2$ collision on the collision energy for $E_T$ = 63,944 $cm^{-1}$, which corresponds to the vibrational energy of each bond only 0.5 eV below the dissociation threshold. As shown in this Figure, the dissociation probability of C-$H_{methyl}$ bond is always larger than that of C-$H_{ring}$. At $E$ = 2 eV, $P_{C\text{-}Hmethyl}$ is as large as 0.0314, whereas $P_{C\text{-}Hring}$ is only 0.0208. At such high collision

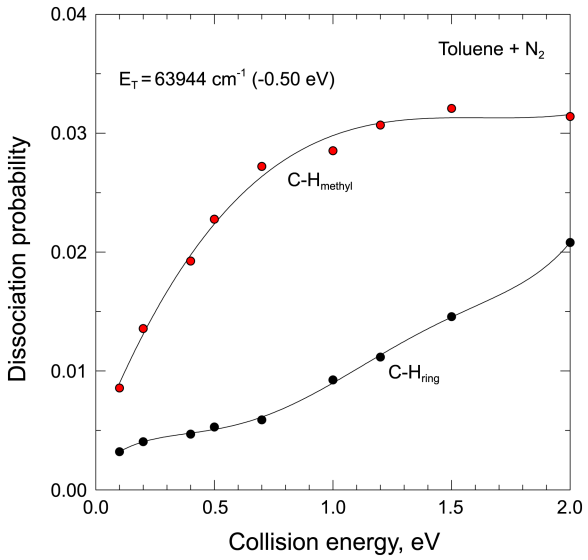


**Figure 7.** Dissociation probabilities of C-$H_{methyl}$ and C-$H_{ring}$ bonds against the collision energy for the total vibrational energy content $E_T$ = 63,944 $cm^{-1}$ for toluene+$N_2$ collision.

energies, where $N_2$ approaches very close to toluene, the incident molecule can maintain a near-collinear alignment with C-$H_{methyl}$ for efficient perturbation (see Figure 2). As can be seen in Figure 2, such alignment is not possible for C-$H_{ring}$ at close range. For $E_T$ = 63,944 $cm^{-1}$, which corresponds to the vibrational energy of each bond only 0.5 eV below the dissociation threshold, the frequecncy of highly excited C-$H_{methyl}$ vibration is 1,075 $cm^{-1}$ while C-$H_{ring}$ frequency is 991 $cm^{-1}$. The overtone frequency of the C-$H_{methyl}$ frequency, 2,150 $cm^{-1}$, is close to the frequency of colliding $N_2$ molecule, 2,358 $cm^{-1}$, rather than that of the C-$H_{ring}$ frequency, 1,982 $cm^{-1}$. Thus, the C-$H_{methyl}$ bond is more strongly perturbed by incident $N_2$ molecule, finally the dissociation probability of C-$H_{methyl}$ bond is larger than that of C-$H_{ring}$. As the similar point of view, the fact of that $P_{C\text{-}Hmethyl}$ is less than $P_{C\text{-}Hring}$ when the total energy content is 70,396 $cm^{-1}$ can be interpreted. For $E_T$ = 70,396 $cm^{-1}$, the overtone of the frequecncy of highly excited C-$H_{methyl}$ vibration, 2,390 $cm^{-1}$, is close to the frequency of colliding $N_2$ molecule rather than that of the C-$H_{methyl}$ frequency, 2,418 $cm^{-1}$. In Figure 8, we show the dependence of the dissociation probabilities of C-H bonds for $O_2$ on the collision energy for $E_T$ = 63,944 $cm^{-1}$ as the same as Figure 7. As shown in these Figures 7 and 8, the C-H bond dissociation probabilities for $N_2$ collider are always greater than for $O_2$ molecule. Furthermore, the dissociation probability of C-$H_{methyl}$ bond is also larger than that of C-$H_{ring}$, which is the same as for toluene+$N_2$ collision. This trend can also be interpreted by the frequency difference as mentioned above.

**Dynamics of Bond Dissociation:** All C-H dissociative events occur in a direct collision on a subpicosecond time scale for both collision systems, toluene+$O_2$ and toluene+$N_2$. Such direct-mode dissociative event for $E_T$ = 63,944 $cm^{-1}$, which corresponds to the vibrational energy of each bond only 0.5 eV below the dissociation threshold, is represented

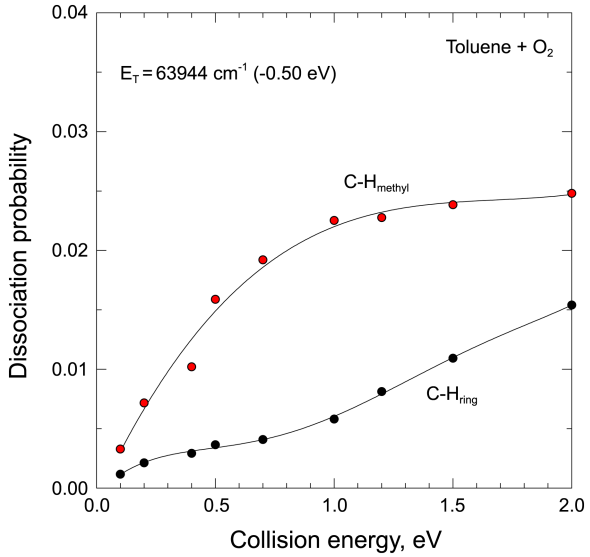


**Figure 8.** Dissociation probabilities of C-$H_{methyl}$ and C-$H_{ring}$ bonds against the collision energy for the total vibrational energy content $E_T$ = 63,944 cm$^{-1}$ for toluene+$O_2$ collision.

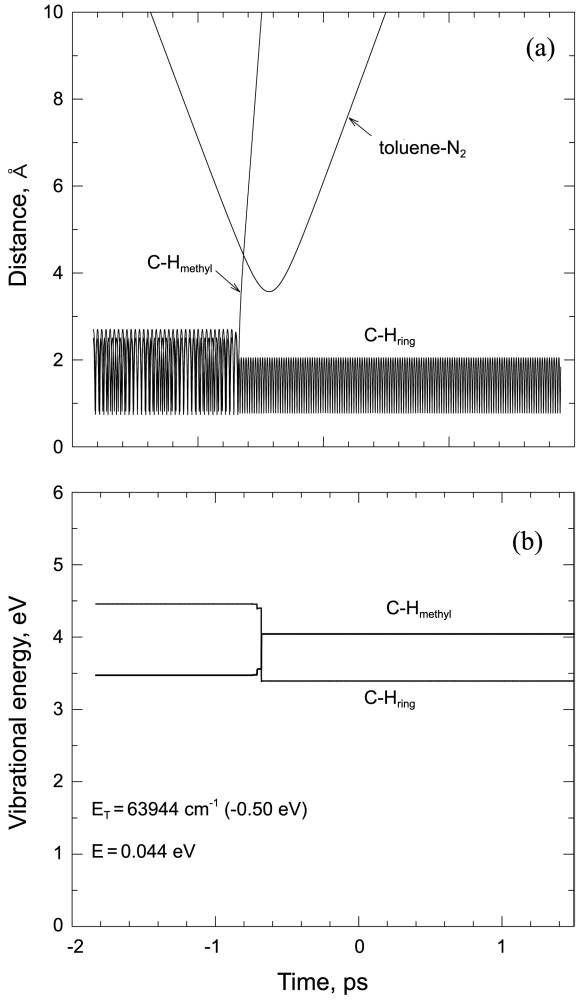


**Figure 9.** Dynamics of the trajectory representing the C-$H_{methyl}$ direct-mode dissociation of toluene with $E_T$ = 63,944 cm$^{-1}$ for toluene+$N_2$ collision. (a) Time evolution of the collision trajectory and C-$H_{ring}$ and C-$H_{methyl}$ bonds. In the collision trajectory, the incoming segment of the toluene-$N_2$ distance is the distance between c.m. of toluene and c.m. of incoming $N_2$ molecule, and its outgoing segment is the distance between c.m. of benzyl radical and c.m. of outgoing $N_2$ molecule. (b) Vibrational energies of C-$H_{ring}$ and C-$H_{methyl}$.

by a typical case shown in Figure 9 for toluene+$N_2$ collision system. We note that the incoming segment of the toluene-$N_2$ distance is the collision trajectory (that is, the distance between c.m. of toluene and c.m. of incoming $N_2$ molecule) and its outgoing segment after reaching the distance of closest approach is the distance between c.m. of benzyl radical and c.m. of outgoing $N_2$ molecule. In this case the closest approach of $N_2$ to the molecule is very close to 3.6 occuring near $t$ = –0.4 ps. The C-$H_{methyl}$ and C-$H_{ring}$ bonds start out the collision process with the frequencies 1,075 and 991 cm$^{-1}$, respectively. At the end of collision, the C-$H_{ring}$ vibration relaxes to the state with the frequency 1,769 cm$^{-1}$. Intramolecular energy flow between the C-H bonds is seen in Figure 9(b), where the time evolution of the vibrational energies of C-$H_{methyl}$ and C-$H_{ring}$ is shown. As shown in this Figure, the C-$H_{ring}$ vibration loses 1.064 eV on collision, while the C-$H_{methyl}$ gains 0.570 eV, indicating an extensive flow of energy between the C-H bonds. For this trajectory $E$ = 0.044 eV and the amount of energy from toluene to $N_2$ is = –0.036 eV. That is, in this trajectory, incident $N_2$ molecule rather transfers energy to toluene. Thus, the total reaction energy available for intramolecular energy flow is (1.064 eV + 0.036 eV) = 1.100 eV. Upon collision with $N_2$, the C-$H_{methyl}$ bond takes the bulk of this energy (0.570 eV) and exceeds the dissociation threshold 3.972 eV. The remaining energy 0.530 eV deposits mainly in the C-C-$H_{ring}$ bend. Figure 10 shows the power spectrum obtained from the Fourier transform of the C-$H_{ring}$ vibration in the excited toluene considered in Figure 9. Two low-frequency main peaks are appearing at 991 and 1,769 cm$^{-1}$, reflecting the before and after collision fundamental frequencies of C-$H_{ring}$ vibration as mentioned above. In this Figure, three minor frequencies, 1,982, 2,983 and 3,529 cm$^{-1}$, are also shown. First two ones are the overtones for the before collision frequency, 991 cm$^{-1}$, and the last one is the overtone for the after collision frequency, 1,769 cm$^{-1}$. Among these frequencies, 1,982 cm$^{-1}$ is close to 2,358 cm$^{-1}$, the frequency of the incident $N_2$ molecule, thus C-$H_{ring}$ can be perturbed effectively by the incident $N_2$ molecule.

Figure 11 shows also the representative direct-mode dissociative event now for toluene+$O_2$ collision system for $E_T$ = 63,944 cm$^{-1}$ as the same as Figure 9 for toluene+$N_2$ collision. For this trajectory $E$ = 0.051 eV and toluene transfers 0.001 eV to $N_2$. The amount of energy lost by the relaxing C-$H_{ring}$ is 0.587 eV (see Figure 11(b)), thus the total reaction energy available for intramolecular energy flow is (0.587 eV–0.001 eV) = 0.586 eV. Upon collision with $O_2$, the C-$H_{methyl}$ bond takes the bulk of this energy (0.531 eV) and exceeds the dissociation threshold 3.972 eV. Figure 12 shows also the power spectrum obtained from the Fourier transform of the C-$H_{ring}$ vibration. The main peaks are ap-

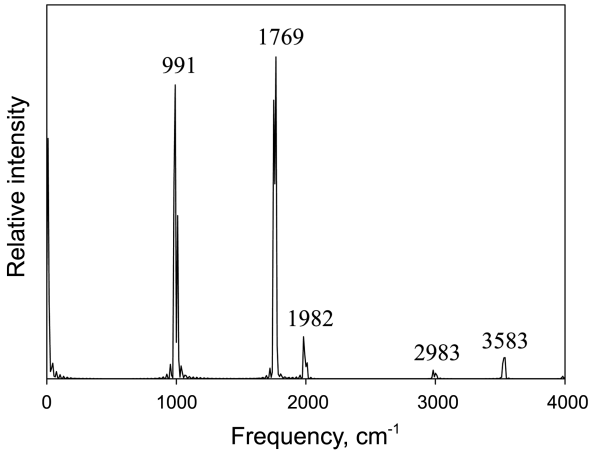


**Figure 10.** Power spectrum obtained from the C-$H_{ring}$ vibration for the trajectory considered in Figure 9.

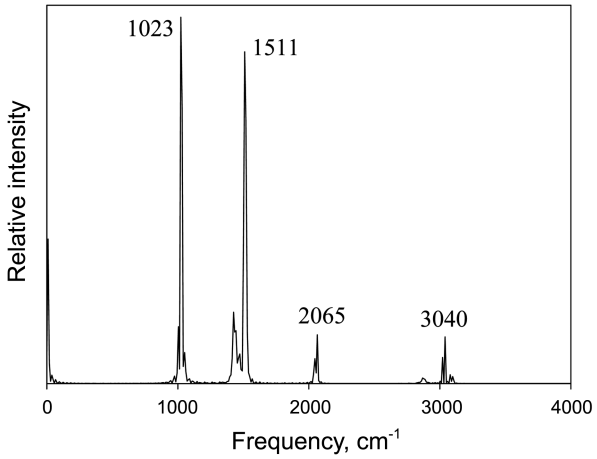


**Figure 12.** Power spectrum obtained from the C-$H_{ring}$ vibration for the trajectory considered in Figure 11.

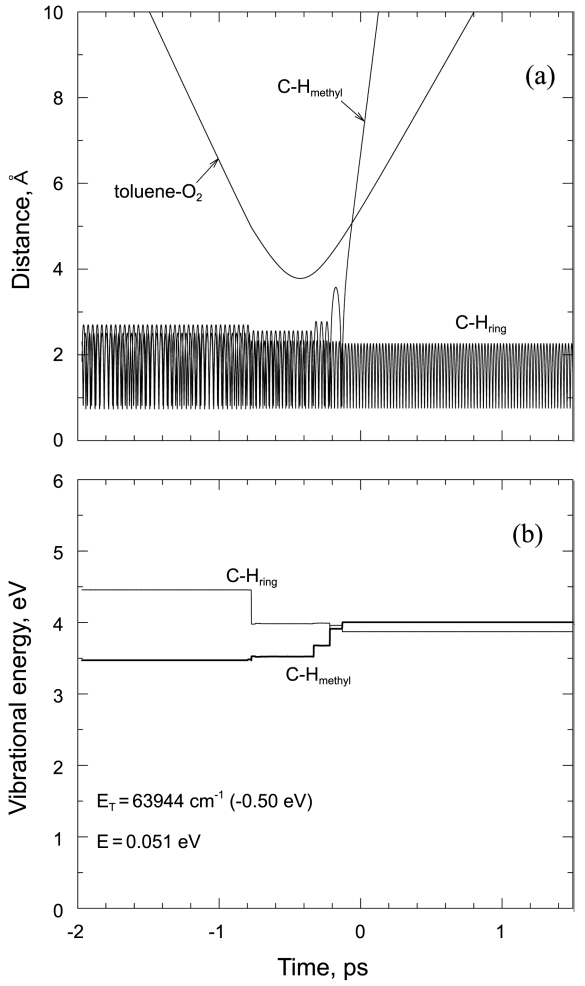


**Figure 11.** Dynamics of the trajectory representing the C-$H_{methyl}$ direct-mode dissociation of toluene with $E_T$ = 63,944 $cm^{-1}$ for toluene+$O_2$ collision. (a) Time evolution of the collision trajectory and C-$H_{ring}$ and C-$H_{methyl}$ bonds. In the collision trajectory, the incoming segment of the toluene-$O_2$ distance is the distance between c.m. of toluene and c.m. of incoming $O_2$ molecule, and its outgoing segment is the distance between c.m. of benzyl radical and c.m. of outgoing $O_2$ molecule. (b) Vibrational energies of C-$H_{ring}$ and C-$H_{methyl}$.

pearing at 1,023 and 1,511 $cm^{-1}$, reflecting the frequencies of highly excited C-$H_{ring}$ vibration before and after the collision, respectively. In this Figure, the bands, 2,065 and 3,040 $cm^{-1}$, are also shown, at which the former is the overtone of C-$H_{ring}$ vibration before the collision and the latter is that after the collision. Two frequencies before the collison, 1,023 and 2,065 $cm^{-1}$ are not quite close to 1,580 $cm^{-1}$, the frequency of the incident $O_2$ molecule, thus C-$H_{methyl}$ dissociation are less than for the toluene+$N_2$ collision. Although only the dissociations of C-$H_{methyl}$ are considered in Figures 9 and 11, C-$H_{ring}$ dissociation events can be discussed similarly.

## Concluding Comments

We have studied CH bond dissociation and intermolecular energy transfer in the toluene-$N_2$ and $O_2$ collision system at 300 K using classical trajectory procedures. The collision system consists of the interaction zone, where the incident molecule interacts with both $CH_{methyl}$ and $CH_{ring}$ bonds, and the inner zone which includes the stretches and bends of toluene beyond the interaction zone.

Energy loss is found to be small, but slowly increases with the total vibrational energy content initially stored in the C-$H_{methyl}$ bond and the adjacent C-$H_{ring}$ bond between 5,000 and 45,000 $cm^{-1}$. The $E_T$ dependence and the magnitude of $-\langle\Delta E\rangle$ of the toluene+$N_2$ and toluene+$O_2$ collisions below 40,000 $cm^{-1}$ agree fairly well with the observed data.[25,27] Intermolecular energy transfer occurs via both of $V \rightarrow T$ and $V \rightarrow V$ transfers, and $V \rightarrow R$ transfer is not significant. Both of $V \rightarrow T$ and $V \rightarrow V$ transfers increase as the total vibrational energy of toluene increases. When the total energy content $E_T$ of toluene is sufficiently high, either C-H bond can dissociate. When the vibrational energies of both C-H bonds are set initially below the dissociation threshold by the same amount, the dissociation probability of C-$H_{methyl}$ bond is found to be larger than that of C-$H_{ring}$ bond, and that in the collision with $N_2$ is larger than with $O_2$. This is can be interpreted by the frequency difference. The overtone for the

before collision frequency of highly excited C-$H_{methyl}$ vibration, 2,150 $cm^{-1}$, is close to the frequency of colliding $N_2$ molecule, 2,358 $cm^{-1}$, rather than that of the C-$H_{ring}$ frequency, 1,982 $cm^{-1}$. Thus, the C-$H_{methyl}$ bond is more strongly perturbed by incident $N_2$ molecule, finally the dissociation probability of C-$H_{methyl}$ bond is larger than that of C-$H_{ring}$. As the similar point of view, the fact of that $P_{C\text{-}Hmethyl}$ is less than $P_{C\text{-}Hring}$ when the total energy content is 70,396 $cm^{-1}$ can be interpreted. These dissociation probabilities are comparable with that for toluene+HBr collision,[26] while are smaller than for HF or Ar colliders.[32,33(c)] Although the extent of energy lost by excited toluene is not large, intramolecular vibrational energy flow between the C-H bonds is very efficient to contribute the C-H bond dissociation and takes place on a subpicosecond time scale.

**Acknowledgments.** This work was financially supported by research fund of Chonnam National University in 2012. J. Ree greatly appreciate to Professor Min Joo Lee for very helpful comments.

## References

1. Yardley, J. T. *Introduction to Molecular Energy Transfer*; Academic: New York, 1980.
2. Zellweger, J. M.; Brown, T. C.; Barker, J. R. *J. Chem. Phys.* **1985**, *83*, 6261.
3. Shi, J.; Barker, J. R. *J. Chem. Phys.* **1988**, *88*, 6219.
4. Yerram, M. L.; Brenner, J. D.; King, K. D.; Barker, J. R. *J. Phys. Chem.* **1990**, *94*, 6341.
5. Hippler, H.; Otto, B.; Troe, J. *Ber. Bunsen-Ges. Phys. Chem.* **1989**, *93*, 428.
6. Nakashima, N.; Yoshihara, K. *J. Chem. Phys.* **1983**, *79*, 2727.
7. Abel, B.; Herzog, B.; Hippler, H.; Troe, J. *J. Chem. Phys*. **1989**, *91*, 900.
8. Heymann, M.; Hippler, H.; Nahr, D.; Plach, H. J.; Troe, J. *J. Phys. Chem.* **1988**, *92*, 5507.
9. Heymann, M.; Hippler, H.; Plach, H. J.; Troe, J. *J. Chem. Phys.* **1987**, *87*, 3867.
10. Wallington, T. J.; Scheer, M. D.; Braun, W. *Chem. Phys. Lett.* **1987**, *138*, 538.
11. Beck, K. M.; Gordon, R. J. *J. Chem. Phys.* **1987**, *87*, 5681.
12. Toselli, B. M.; Walunas, T. L.; Barker, J. R. *J. Chem. Phys.* **1990**, *92*, 4793.
13. Clary, D. C.; Gilbert, R. G.; Bernshtein, V.; Oref, I. *Faraday Discuss.* **1995**, *102*, 423.
14. Sevy, E. T.; Rubin, S. M.; Lin, Z.; Flynn, G. W. *J. Chem. Phys.* **2000**, *113*, 4912.
15. Ree, J.; Kim, Y. H.; Shin, H. K. *J. Chem. Phys.* **2002**, *116*, 4858.
16. Du, J.; Yuan, L.; Hsieh, S.; Lin, F.; Mullin, A. S. *J. Phys. Chem. A* **2008**, *112*, 9396.
17. For a review, see Hsu, H. C.; Tsai, M.-T.; Dyakov, Y. A.; Ni, C.-K. *Int. Rev. Phys. Chem.* **2012**, *31*, 201.
18. Schwartz, R. N.; Slawsky, Z. I.; Herzfeld, K. F. *J. Chem. Phys.* **1952**, *20*, 1591.
19. Tanczos, F. I. *J. Chem. Phys.* **1956**, *25*, 439.
20. Schranz, H. W.; Nordholm, S. *Int. J. Chem. Kinet.* **1981**, *13*, 1051.
21. Gilbert, R. G. *J. Chem. Phys.* **1984**, *80*, 5501.
22. (a) Sceats, M. G. *J. Chem. Phys.* **1989**, *91*, 6795. (b) Hynes R. G.; Sceats, M. G. *ibid.* **1989**, *91*, 6804.
23. Toselli, B. M.; Barker, J. R. *Chem. Phys. Lett.* **1990**, *174*, 304.
24. Lim, K. F.; Gilbert, R. G. *J. Phys. Chem.* **1990**, *94*, 72; **1990**, *94*, 77.
25. Toselli, B. M.; Brenner, J. D.; Yerram, M. L.; Chin, W. E.; King, K. D.; Barker, J. R. *J. Chem. Phys.* **1991**, *95*, 176.
26. Lee, S.; Ree, J. *Bull. Kor. Chem. Soc.* **2012**, *33*, 1063.
27. Wright, S. M. A.; Sims, I. R.; Smith, I. W. M. *J. Phys. Chem. A* **2000**, *104*, 10347.
28. Lim, K. F. *J. Chem. Phys.* **1994**, *101*, 8756.
29. Catlett, D. L., Jr.; Parmenter, C. S.; Pursell, C. J. *J. Phys. Chem.* **1994**, *98*, 3263; *ibid.* **1995**, *99*, 7371.
30. Shin, H. K. *J. Phys. Chem. A* **2000**, *104*, 6699.
31. Nilsson, D.; Nordholm, S. *J. Chem. Phys.* **2002**, *116*, 7040.
32. Ree, J.; Kim, Y. H.; Shin, H. K. *Chem. Phys. Lett.* **2004**, *394*, 250.
33. (a) Ree, J.; Chang, K. S.; Kim, Y. H.; Shin, H. K. *Bull. Kor. Chem. Soc.* **2003**, *24*, 1223. (b) Ree, J.; Kim, Y. H.; Shin, H. K. *ibid.* **2005**, *26*, 1269. (c) Ree, J.; Kim, S. H.; Lee, T. H.; Kim, Y. H. *ibid.* **2006**, *27*, 495.
34. (a) Hippler, H.; Troe, J.; Wendelken, H. J. *Chem. Phys. Lett.* **1981**, *84*, 257. (b) *J. Chem. Phys.* **1983**, *78*, 5351; *78*, 6709; *78*, 6718 (c) **1984**, *80*, 1853.
35. (a) Bernshtein, V.; Oref. I. *J. Phys. Chem. A* **2006**, *110*, 8477. (b) *J. Phys. Chem. B* **2005**, *109*, 8310. (c) *J. Phys. Chem. A* **2006**, *110*, 1541.
36. Hirschfelder, J. O.; Curtiss, C. F.; Bird, R. B. *Molecular Theory of Gases and Liquids*; Wiley: New York, 1967; see p. 168 for the combining laws, pp 1110-1112 and 1212-1214 for D and σ, respectively.
37. Lim, K. F. *J. Chem. Phys.* **1994**, *100*, 7385.
38. Xie, Y.; Boggs, J. E. *J. Comp. Chem.* **1986**, *7*, 158.
39. http://webbook.nist.gov/chemistry/name-ser.html
40. Olney, T. N.; Cann, N. M.; Cooper, G.; Brion, C. E. *Chem. Phys.* **1997**, *223*, 59.
41. Huber, K. P.; Herzberg, G. *Constants of Diatomic Molecules*; Van Nostrand Reinhold: New York, 1979.
42. Gear, C. W. *Numerical Initial Value Problems in Ordinary Differential Equations*; Prentice-Hall: New York, 1971.
43. MATH/LIBRARY, *Fortran Subroutines for Mathematical Applications*; IMSL: Houston, 1989; p 640.